

# EXPERIMENTAL INPUTS TO THE STANDARD MODEL PREDICTION OF $(g - 2)_\mu^*$

THOMAS LENZ

on behalf of the BESIII Collaboration

Johannes Gutenberg University, Mainz, Germany

*Received 23 December 2021, accepted 28 December 2021,  
published online 28 February 2022*

A deviation of  $4.2\sigma$ , between the experimental measurement and the theoretical determination of the anomalous magnetic moment of the muon  $a_\mu = (g - 2)_\mu/2$ , has been observed. With increased experimental precision expected in the near future, the theoretical prediction within the Standard Model also needs to be improved. Its total uncertainty is limited by the two hadronic contributions, namely the hadronic vacuum polarization and the hadronic light-by-light contribution. The BESIII experiment at the BEPCII accelerator offers the largest datasets in the  $\tau$ -charm energy region and is, therefore, perfectly suited to provide cross section and form factor measurements in  $e^+e^-$  collisions for data-driven improvements of the Standard Model prediction.

DOI:10.5506/APhysPolBSupp.15.2-A1

## 1. The anomalous magnetic moment of the muon

The anomalous magnetic moment of the muon represents a precision test of the Standard Model of particle physics. The  $a_\mu = (g - 2)_\mu/2$  anomaly is defined as the relative deviation from the value predicted in the Dirac theory [1]. The experimental measurement has a long history and its precision has been increased by several orders of magnitude to this day. The latest measurements are from BNL [2] and FNAL [3], which both agree well within their uncertainties. However, the average value deviates by  $4.2\sigma$  from the Standard Model prediction of the Muon  $(g - 2)$  Theory Initiative [4].

In the future, FNAL will use larger datasets to reduce the statistical uncertainty and the Muon  $(g - 2)/\text{EDM}$  experiment at J-PARC [5] will provide a complementary measurement, relying on a different approach, to even further improve the results.

---

\* Presented at the XLIV International Conference of Theoretical Physics “Matter to the Deepest”, 15–17 September, 2021.

### 1.1. Standard Model prediction

The Standard Model prediction can be divided into four separate contributions: Quantum Electrodynamics (QED), weak interactions, hadronic vacuum polarization (HVP), and hadronic light-by-light scattering (HLbL). As listed in Table 1, the QED contribution is leading the total value of  $a_\mu$  by several orders of magnitude, while having the smallest contribution to the overall uncertainty [6, 7]. Also, the electroweak contribution is known to a good precision [8, 9]. However, due to the non-perturbative nature of Quantum Chromodynamics (QCD), the two hadronic contributions cannot be treated perturbatively and are dominating the total uncertainty.

Table 1. Contributions to the Standard Model prediction of  $a_\mu$  [4].

Contribution	$a_\mu \times 10^{11}$	Ref.
QED	116 584 718.931 ± 0.104	[6, 7]
Electroweak	153.6 ± 1.0	[8, 9]
HVP	6845 ± 40	[10–16]
HLbL	92 ± 18	[17–31]
Total	116 591 810	± 43

#### 1.1.1. Hadronic vacuum polarization

The dominating hadronic contribution is HVP. With a dispersive approach, the leading-order contribution  $a_\mu^{\text{HVP,LO}}$  can be directly related to the hadronic cross sections  $\sigma_{\text{had}}(s)$  measured in  $e^+e^-$  annihilations and a known kernel function  $K(s)$ , where  $s$  is the squared center-of-mass energy [10–16]

$$a_\mu^{\text{HVP,LO}} = \frac{1}{4\pi} \int_{m_\pi^2}^{\infty} ds K(s) \sigma_{\text{had}}(s). \quad (1)$$

Since both the hadronic cross section and the kernel function scale with  $1/s$ , the total value of  $a_\mu^{\text{HVP,LO}}$  is dominated by very low energies. This can also be seen in Table 2(a), where the lowest multiplicity state  $\pi^+\pi^-$  contributes by an order of magnitude more than the next higher multiplicity.

#### 1.1.2. Hadronic light-by-light scattering

Recently, data-driven dispersive approaches have also been proposed for the most important sub-graphs of HLbL [19, 24, 32, 33]. However, the relation is not as straightforward. The coupling of four photons to (virtual) hadronic intermediate states can be divided into different contributions. HLbL contributions are also dominated by low momentum transfers  $Q^2$  [17–31].

As listed in Table 2(b), the dominating contributions are the pseudoscalar meson poles ( $\pi^0, \eta, \eta'$ ), due to their strong coupling to two photons. Smaller contributions arise from scalar, vector, and tensor poles as well as hadron and quark loops.

Table 2. Hadronic contributions to the Standard Model prediction of  $a_\mu$ .

(a) HVP (leading order) [15].		(b) HLbL [17–31].	
Contribution	$a_\mu^{\text{HVP,LO}} \times 10^{11}$	Contribution	$a_\mu^{\text{HLbL}} \times 10^{11}$
$\pi^+ \pi^-$	$5042.3 \pm 19.0$	$\pi^0, \eta, \eta'$ -poles	$93.8 \pm 4.0$
$\pi^+ \pi^- \pi^0$	$466.3 \pm 9.4$	$\pi, K$ -loops/boxes	$-16.4 \pm 0.2$
$\pi^+ \pi^- \pi^0 \pi^0$	$181.5 \pm 7.4$	$S$ -wave $\pi\pi$	$-8 \pm 1$
$\pi^+ \pi^- \pi^+ \pi^-$	$139.9 \pm 1.9$	rescattering	
$K^+ K^-$	$230.0 \pm 2.2$	Scalars & tensors	$-1 \pm 3$
$K_S^0 K_L^0$	$130.4 \pm 1.9$	Axial vectors	$6 \pm 6$
$\pi^0 \gamma$	$45.8 \pm 1.0$	$u, d, s$ -loops / short distance	$15 \pm 10$
1.8–3.7 GeV (without $c\bar{c}$ )	$344.5 \pm 5.6$	$c$ -loop	$3 \pm 1$
$J/\psi, \psi(2S)$	$78.4 \pm 1.9$	Total	$92 \pm 19$
$\geq 3.7$ GeV	$169.5 \pm 1.9$		
Total	$6928 \pm 24$		

## 2. The BESIII experiment

The BESIII experiment [34] is located at the BEPCII accelerator, which is a symmetric  $e^+e^-$  collider in Beijing, China. The center-of-mass energy  $\sqrt{s}$  ranges from 2 GeV to 5 GeV, and in 2016 its design luminosity of  $10^{33} \text{ cm}^{-2} \text{ s}^{-1}$  has been reached. The BESIII detector is a  $4\pi$  detector, which covers 93% of the solid angle. It contains a drift chamber in an axial 1 T magnetic field, a time-of-flight system, an electromagnetic calorimeter, and a muon counter.

BESIII offers world-leading data sets in the  $\tau$ -charm energy region with over  $10^{10}$   $J/\psi$  events and other large data sets collected at further charmonium resonances and in the mass range of charmonium-like  $XYZ$  particles. Additionally, there are over 130 energy scan points in the range from 2.0 GeV to 4.6 GeV with at least  $10^5$  hadronic events each.

## 3. HVP measurements

As mentioned before,  $a_\mu^{\text{HVP}}$  is dominated by processes at energies below 1 GeV. Since these energies are out of reach for the BEPCII accelerator, at BESIII, the measurements of the hadronic cross section in the relevant

energy region rely on the initial-state radiation (ISR) technique. Here, one of the initial  $e^\pm$  emits a photon and, therefore, lowers the effective center-of-mass energy  $\sqrt{s'}$ . Since the emission of an ISR photon is a higher-order QED process, very large statistics are required to perform a high-precision measurement.

### 3.1. $e^+e^- \rightarrow \pi^+\pi^-$

The  $e^+e^- \rightarrow \pi^+\pi^-$  channel has by far the largest contribution to  $a_\mu^{\text{HVP}}$  (see Table 2(a)). Therefore, it is of utmost importance to measure the cross section with high precision, especially in the region of the  $\rho(770)^0$  and  $\omega(782)$  resonances from 0.6 GeV to 0.9 GeV. This region alone makes up 50% of the leading order contribution of  $a_\mu^{\text{HVP}}$ .

The world leading measurements from BaBar [39] and KLOE [41], with 0.7% and 0.6% precision, respectively, are in tension with each other (see Fig. 1(b)). Based on the  $2.9\text{ fb}^{-1}$  data set at 3.773 GeV, BESIII [35] has measured the cross section using the ISR technique with 1.0% precision (see Fig. 1(a)). Currently, BESIII is carrying out new analyses, which aim at

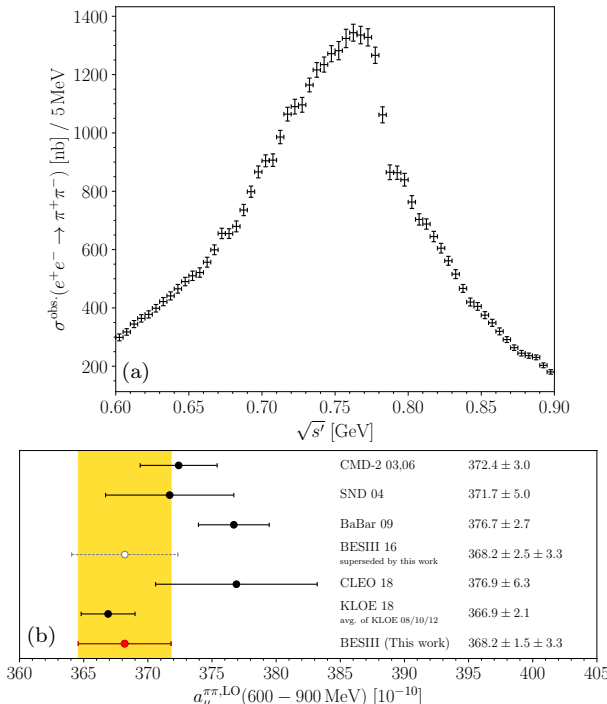


Fig. 1. (a) Cross-section measurement of  $e^+e^- \rightarrow \pi^+\pi^-$  in the  $\rho(770)^0 - \omega(782)$  region from BESIII [35] and (b) a comparison of  $a_\mu^{\pi\pi}$  evaluations in the range from 0.6 GeV to 0.9 GeV using different cross-section measurements [35–41].

a precision of 0.5%. This will be achieved using  $20 \text{ fb}^{-1}$  of data, which are going to be collected in the upcoming data taking period, at  $3.773 \text{ GeV}$ , a normalization to the muon yield, and an improved  $\pi - \mu$  separation. Additionally, a good understanding of the radiative corrections [42] is necessary to achieve such high precisions.

### 3.2. $e^+e^- \rightarrow \pi^+\pi^-\pi^0(\pi^0)$

The  $\pi^+\pi^-\pi^0$  and  $\pi^+\pi^-\pi^0\pi^0$  channels give rise to the next largest contributions to  $a_\mu^{\text{HVP}}$  and also their uncertainties. BESIII [43, 44], and also BaBar [45, 46], have measured the cross section of both channels using the ISR technique. This technique offers the coverage of the whole mass range with unprecedented precision compared to scan measurements (see Fig. 2). The  $3\pi$  measurement at BESIII has reached 1% precision [43] and the  $4\pi$  measurement reached 3% [44]. Both measurements are limited by the statistical uncertainty and will be improved with the upcoming data set of  $20 \text{ fb}^{-1}$  at  $3.773 \text{ GeV}$ . The main background for both channels is due to an additional  $\pi^0$  and thus the analyses share large synergies.

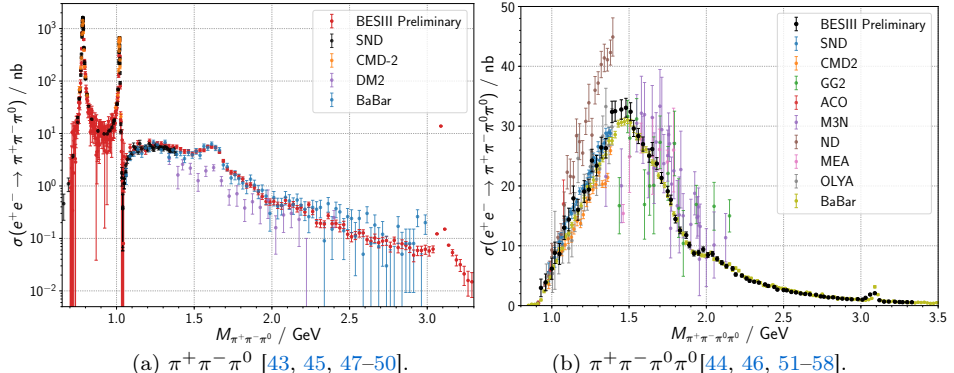


Fig. 2. Cross-section measurements of the respective channels.

### 3.3. $e^+e^- \rightarrow \text{hadrons}$

BESIII is also carrying out an inclusive measurement of the cross section  $e^+e^- \rightarrow \text{hadrons}$ . For this, currently, 14 scan points between  $2.2 \text{ GeV}$  and  $3.7 \text{ GeV}$  are used with at least  $10^5$  hadronic events each. The result is relying on precise Monte Carlo generators to evaluate backgrounds events and the tagging efficiency of hadronic events. The measurement is aiming at 3% precision [59], surpassing the measurement from BES (6%) [60].

#### 4. HLbL measurements

Two-photon interactions can be probed at  $e^+e^-$  colliders using the  $e^+e^- \rightarrow e^+e^-\gamma^{(*)}\gamma^{(*)} \rightarrow e^+e^-X$  reaction. The cross section of the process is directly proportional to the transition form factor (TFF)  $|\mathcal{F}_X(q_1^2, q_2^2)|^2$ , where  $q_1^2, q_2^2$  are the momentum transfers of the (virtual) photons, and to the center-of-mass energy  $\sqrt{s}$

$$\sigma(e^+e^- \rightarrow e^+e^-X) \propto |\mathcal{F}_X(q_1^2, q_2^2)|^2 \alpha^2 \ln^2 \sqrt{s}. \quad (2)$$

Similar to ISR, two-photon physics has very forward-peaked kinematics, favoring small scattering angles of the  $e^\pm$ . This leads to three different analysis strategies: the untagged measurement assumes  $q_1^2 = q_2^2 \approx 0$  and does not detect any of the scattered leptons, the single-tag measurement detects one scattered lepton ( $q_1^2 \neq 0, q_2^2 \approx 0$ ), and the double-tag measurement both ( $q_1^2, q_2^2 \neq 0$ ).

##### 4.1. $\gamma\gamma^* \rightarrow \pi^0, \eta, \eta'$

The  $\pi^0$  single-virtual space-like TFF  $\mathcal{F}_{\pi^0}(Q^2, 0)$ , depending on  $Q^2 = -q^2$ , has been measured by CELLO [61], CLEO [62], BaBar [63], and Belle [64]. BESIII offers the opportunity to perform a single-tag measurement with unprecedented precision in the most relevant  $Q^2$  region for  $a_\mu^{\text{HLbL}}$  using  $2.9 \text{ fb}^{-1}$  of data at  $3.773 \text{ GeV}$ . As depicted in Fig. 3 (a), preliminary results from BESIII [65] are in good agreement with dispersive calculations [66] and lattice QCD simulations [21] of the TFF. Additionally to the  $\pi^0$ , BESIII also performs the analysis of the  $\eta$  and  $\eta'$  TFF.

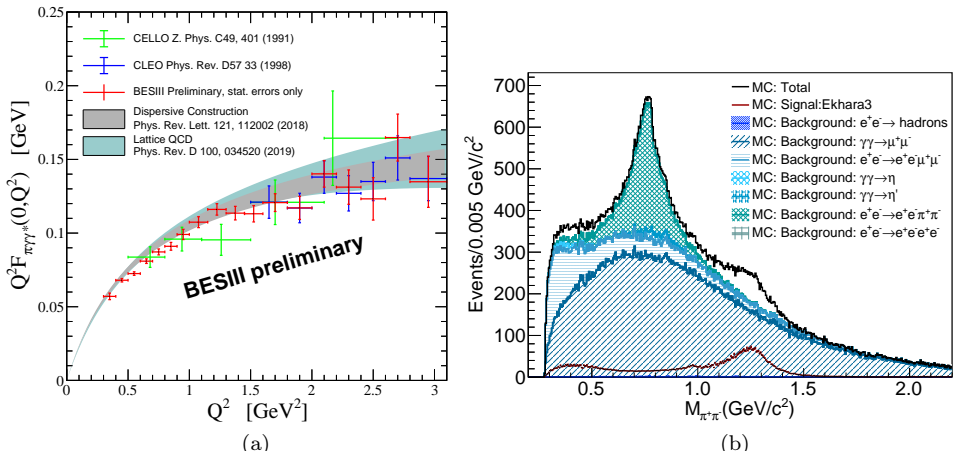


Fig. 3. (a) Comparison of the single-virtual space-like  $\pi^0$  TFF measurements [61, 62, 65] with the dispersive reconstruction [66] and lattice QCD simulations [21] and (b) simulations of the measurement of  $e^+e^- \rightarrow e^+e^-\pi^+\pi^-$  at  $4.23 \text{ GeV}$  with signal and background contributions [67].

#### 4.2. $\gamma\gamma^* \rightarrow \pi^+\pi^-$

The measurement of  $e^+e^- \rightarrow e^+e^-\pi^+\pi^-$  offers input for the contributions of  $\pi$ -loops and boxes,  $S$ -wave  $\pi\pi$  rescattering, and scalar and tensor states (see Table 2 (b)).

The single-tag analysis is dominated by reducible background from  $e^+e^- \rightarrow e^+e^-\mu^+\mu^-$ , which can be removed with precise knowledge of all amplitudes and their interferences and a refined  $\pi\mu$  separation using machine learning tools. Radiative Bhabha scattering, where the emitted photon couples to a  $\rho(770)^0$  meson, is an irreducible background. Also here, the knowledge of all amplitudes and their interferences is very important [68]. The measurement at BESIII provides a coverage of the mass range from the threshold to 2 GeV (see Fig. 3 (b)), of the momentum transfer from 0.2  $\text{GeV}^2$  to 2  $\text{GeV}^2$ , and of the full helicity angle [67].

#### 4.3. Higher meson multiplicities

To help the understanding of the contributions from axial vector and tensor mesons, BESIII is carrying out analyses of the processes like  $\gamma\gamma^* \rightarrow \pi^+\pi^-\pi^0$ ,  $\gamma\gamma^* \rightarrow \pi^+\pi^-\eta$ ,  $\gamma\gamma^* \rightarrow K\bar{K}\pi$ , and  $\gamma\gamma^* \rightarrow f_1(1285)$ .

A single-tag measurement of  $\gamma\gamma^* \rightarrow \pi^0\pi^0, \pi^0\eta$  will produce results in a complementary  $Q^2$  range to Belle [69], and the first double-tag measurement of the  $\pi^0$  TFF with  $\gamma^*\gamma^* \rightarrow \pi^0$  is foreseen for the full future data set.

### 5. Summary

The uncertainty of the Standard Model prediction of the anomalous magnetic moment of the muon is dominated by hadronic contributions. With its large datasets in the  $\tau$ -charm energy region, BESIII offers the opportunity to perform precision measurements, which serve as input for the dispersive evaluations of HVP and HLbL.

For  $a_\mu^{\text{HVP}}$ , BESIII uses the ISR technique to measure the  $\pi^+\pi^-$ ,  $\pi^+\pi^-\pi^0$ , and  $\pi^+\pi^-\pi^0\pi^0$  cross sections in the relevant mass region. Additionally, the inclusive hadronic cross section is scanned from 2.2 GeV to 3.7 GeV.

Two-photon cross section measurements of  $\gamma\gamma^* \rightarrow \pi^0, \eta, \eta'$ ,  $\gamma\gamma^* \rightarrow \pi^+\pi^-$ , and higher meson multiplicities are used for  $a_\mu^{\text{HLbL}}$ .

All measurements discussed here will benefit from the new larger data sets at BESIII, especially from the  $20 \text{ fb}^{-1}$  at 3.773 GeV, which will be collected in the next two years of BESIII.

## REFERENCES

- [1] P.A.M. Dirac, «The quantum theory of the electron», *Proc. Roy. Soc. Lond. A* **117**, 610 (1928).
- [2] G.W. Bennett *et al.*, «Final report of the muon E821 anomalous magnetic moment measurement at BNL», *Phys. Rev. D* **73**, 072003 (2006).
- [3] B. Abi *et al.*, «Measurement of the Positive Muon Anomalous Magnetic Moment to 0.46 ppm», *Phys. Rev. Lett.* **126**, 141801 (2021).
- [4] T. Aoyama *et al.*, «The anomalous magnetic moment of the muon in the Standard Model», *Phys. Rep.* **887**, 1 (2020).
- [5] M. Abe *et al.*, «A new approach for measuring the muon anomalous magnetic moment and electric dipole moment», *Prog. Theor. Exp. Phys.* **2019**, 053C02 (2019).
- [6] T. Aoyama, M. Hayakawa, T. Kinoshita, M. Nio, «Complete Tenth-Order QED Contribution to the Muon  $g - 2$ », *Phys. Rev. Lett.* **109**, 111808 (2012).
- [7] T. Aoyama, T. Kinoshita, M. Nio, «Theory of the Anomalous Magnetic Moment of the Electron», *Atoms* **7**, 28 (2019).
- [8] A. Czarnecki, W.J. Marciano, A. Vainshtein, «Refinements in electroweak contributions to the muon anomalous magnetic moment», *Phys. Rev. D* **67**, 073006 (2003), *Erratum ibid.* **73**, 119901 (2006).
- [9] C. Gnendiger, D. Stöckinger, H. Stöckinger-Kim, «The electroweak contributions to  $(g - 2)_\mu$  after the Higgs boson mass measurement», *Phys. Rev. D* **88**, 053005 (2013).
- [10] M. Davier, A. Hoecker, B. Malaescu, Z. Zhang, «Reevaluation of the hadronic vacuum polarisation contributions to the Standard Model predictions of the muon  $g - 2$  and  $\alpha(m_Z^2)$  using newest hadronic cross-section data», *Eur. Phys. J. C* **77**, 827 (2017).
- [11] A. Keshavarzi, D. Nomura, T. Teubner, «Muon  $g - 2$  and  $\alpha(M_Z^2)$ : A new data-based analysis», *Phys. Rev. D* **97**, 114025 (2018).
- [12] G. Colangelo, M. Hoferichter, P. Stoffer, «Two-pion contribution to hadronic vacuum polarization», *J. High Energy Phys.* **1902**, 6 (2019).
- [13] M. Hoferichter, B.-L. Hoid, B. Kubis, «Three-pion contribution to hadronic vacuum polarization», *J. High Energy Phys.* **1908**, 137 (2019).
- [14] M. Davier, A. Hoecker, B. Malaescu, Z. Zhang, «A new evaluation of the hadronic vacuum polarisation contributions to the muon anomalous magnetic moment and to  $\alpha(m_Z^2)$ », *Eur. Phys. J. C* **80**, 241 (2020), *Erratum ibid.* **80**, 410 (2020).
- [15] A. Keshavarzi, D. Nomura, T. Teubner, « $g - 2$  of charged leptons,  $\alpha(M_Z^2)$  and the hyperfine splitting of muonium», *Phys. Rev. D* **101**, 014029 (2020).
- [16] A. Kurz, T. Liu, P. Marquard, M. Steinhauser, «Hadronic contribution to the muon anomalous magnetic moment to next-to-next-to-leading order», *Phys. Lett. B* **734**, 144 (2014).
- [17] K. Melnikov, A. Vainshtein, «Hadronic light-by-light scattering contribution to the muon anomalous magnetic moment revisited», *Phys. Rev. D* **70**, 113006 (2004).

- [18] P. Masjuan, P. Sánchez-Puertas, «Pseudoscalar-pole contribution to the  $(g_\mu - 2)$ : A rational approach», *Phys. Rev. D* **95**, 054026 (2017).
- [19] G. Colangelo, M. Hoferichter, M. Procura, P. Stoffer, «Dispersion relation for hadronic light-by-light scattering: two-pion contributions», *J. High Energy Phys.* **1704**, 161 (2017).
- [20] M. Hoferichter *et al.*, «Dispersion relation for hadronic light-by-light scattering: pion pole», *J. High Energy Phys.* **1810**, 141 (2018).
- [21] A. Gérardin, H.B. Meyer, A. Nyffeler, «Lattice calculation of the pion transition form factor with  $N_f = 2 + 1$  Wilson quarks», *Phys. Rev. D* **100**, 034520 (2019).
- [22] J. Bijnens, N. Hermansson-Truedsson, A. Rodríguez-Sánchez, «Short-distance constraints for the HLbL contribution to the muon anomalous magnetic moment», *Phys. Lett. B* **798**, 134994 (2019).
- [23] G. Colangelo *et al.*, «Longitudinal short-distance constraints for the hadronic light-by-light contribution to  $(g - 2)_\mu$  with large- $N_c$  Regge models», *J. High Energy Phys.* **2003**, 101 (2020).
- [24] V. Pauk, M. Vanderhaeghen, «Single meson contributions to the muon's anomalous magnetic moment», *Eur. Phys. J. C* **74**, 3008 (2014).
- [25] I. Danilkin, M. Vanderhaeghen, «Light-by-light scattering sum rules in light of new data», *Phys. Rev. D* **95**, 014019 (2017).
- [26] F. Jegerlehner, «The Anomalous Magnetic Moment of the Muon», *Springer Tracts Mod. Phys.* **274**, 1 (2017).
- [27] M. Knecht, S. Narison, A. Rabemananjara, D. Rabetiarivony, «Scalar meson contributions to  $a_\mu$  from hadronic light-by-light scattering», *Phys. Lett. B* **787**, 111 (2018).
- [28] G. Eichmann, C.S. Fischer, R. Williams, «Kaon-box contribution to the anomalous magnetic moment of the muon», *Phys. Rev. D* **101**, 054015 (2020).
- [29] P. Roig, P. Sánchez-Puertas, «Axial-vector exchange contribution to the hadronic light-by-light piece of the muon anomalous magnetic moment», *Phys. Rev. D* **101**, 074019 (2020).
- [30] T. Blum *et al.*, «The Hadronic Light-by-Light Scattering Contribution to the Muon Anomalous Magnetic Moment from Lattice QCD», *Phys. Rev. Lett.* **124**, 132002 (2020).
- [31] G. Colangelo *et al.*, «Remarks on higher-order hadronic corrections to the muon  $g - 2$ », *Phys. Lett. B* **735**, 90 (2014).
- [32] G. Colangelo, M. Hoferichter, M. Procura, P. Stoffer, «Dispersive approach to hadronic light-by-light scattering», *J. High Energy Phys.* **1409**, 91 (2014).
- [33] G. Colangelo, M. Hoferichter, M. Procura, P. Stoffer, «Dispersion relation for hadronic light-by-light scattering: theoretical foundations», *J. High Energy Phys.* **1509**, 74 (2015).
- [34] M. Ablikim *et al.*, «Design and Construction of the BESIII Detector», *Nucl. Instrum. Methods Phys. Res. A* **614**, 345 (2010).

- [35] M. Ablikim *et al.*, «Measurement of the  $e^+e^- \rightarrow \pi^+\pi^-$  cross section between 600 and 900 MeV using initial state radiation», *Phys. Lett. B* **753**, 629 (2016), *Corrigendum ibid.* **812**, 135982 (2021).
- [36] R.R. Akhmetshin *et al.*, «Update: Reanalysis of hadronic cross-section measurements at CMD-2», *Phys. Lett. B* **578**, 285 (2004).
- [37] R.R. Akhmetshin *et al.*, «High-statistics measurement of the pion form factor in the  $\rho$ -meson energy range with the CMD-2 detector», *Phys. Lett. B* **648**, 28 (2007).
- [38] M.N. Achasov *et al.*, «Update of the  $e^+e^- \rightarrow \pi^+\pi^-$  cross-section measured by SND detector in the energy region  $400 \text{ MeV} < \sqrt{s} < 1000 \text{ MeV}$ », *J. Exp. Theor. Phys.* **103**, 380 (2006).
- [39] J.P. Lees *et al.*, «Precise measurement of the  $e^+e^- \rightarrow \pi^+\pi^-(\gamma)$  cross section with the initial-state radiation method at BaBar», *Phys. Rev. D* **86**, 032013 (2012).
- [40] T. Xiao *et al.*, «Precision measurement of the hadronic contribution to the muon anomalous magnetic moment», *Phys. Rev. D* **97**, 032012 (2018).
- [41] A. Anastasi *et al.*, «Combination of KLOE  $\sigma(e^+e^- \rightarrow \pi^+\pi^-\gamma(\gamma))$  measurements and determination of  $a_\mu^{\pi^+\pi^-}$  in the energy range  $0.10 < s < 0.95 \text{ GeV}^2$ », *J. High Energy Phys.* **1803**, 173 (2018).
- [42] F. Campanario *et al.*, «Standard model radiative corrections in the pion form factor measurements do not explain the  $a_\mu$  anomaly», *Phys. Rev. D* **100**, 076004 (2019).
- [43] M. Ablikim *et al.*, «Measurement of the  $e^+e^- \rightarrow \pi^+\pi^-\pi^0$  cross section from 0.7 GeV to 3.0 GeV via initial-state radiation», [arXiv:1912.11208 \[hep-ex\]](https://arxiv.org/abs/1912.11208).
- [44] M. Ripka, «Initial State Radiation Measurements at BESIII», *EPJ Web Conf.* **218**, 02004 (2019).
- [45] B. Aubert *et al.*, «Study of  $e^+e^- \rightarrow \pi^+\pi^-\pi^0$  process using initial state radiation with BaBar», *Phys. Rev. D* **70**, 072004 (2004).
- [46] J.P. Lees *et al.*, «Measurement of the  $e^+e^- \rightarrow \pi^+\pi^-\pi^0\pi^0$  cross section using initial-state radiation at BaBar», *Phys. Rev. D* **96**, 092009 (2017).
- [47] R.R. Akhmetshin *et al.*, «Measurement of omega meson parameters in  $\pi^+\pi^-\pi^0$  decay mode with CMD-2», *Phys. Lett. B* **476**, 33 (2000).
- [48] M.N. Achasov *et al.*, «Study of the process  $e^+e^- \rightarrow \pi^+\pi^-\pi^0$  in the energy region  $\sqrt{s}$  from 0.98 GeV to 1.38 GeV», *Phys. Rev. D* **66**, 032001 (2002).
- [49] A. Antonelli *et al.*, «Measurement of the  $e^+e^- \rightarrow \pi^+\pi^-\pi^0$  and  $e^+e^- \rightarrow \omega\pi^+\pi^-$  reactions in the energy interval 1350 MeV–2400 MeV», *Z. Phys. C* **56**, 15 (1992).
- [50] R.R. Akhmetshin *et al.*, «Study of dynamics of  $\phi \rightarrow \pi^+\pi^-\pi^0$  decay with CMD-2 detector», *Phys. Lett. B* **434**, 426 (1998).
- [51] R.R. Akhmetshin *et al.*, « $a_1(1260)\pi$  dominance in the process  $e^+e^- \rightarrow 4\pi$  at energies 1.05 GeV–1.38 GeV», *Phys. Lett. B* **466**, 392 (1999).
- [52] G. Cosme *et al.*, «Multi-pion production below 1.1 GeV by  $e^+e^-$  annihilation», *Phys. Lett. B* **63**, 349 (1976).

- [53] G. Cosme *et al.*, «Hadronic cross-sections study in  $e^+e^-$  collisions from 1.350 GeV to 2.125 GeV», *Nucl. Phys. B* **152**, 215 (1979).
- [54] B. Esposito *et al.*, «Measurement on  $\pi^+\pi^-\pi^0\pi^0$ ,  $\pi^+\pi^-\pi^+\pi^-\pi^0$ ,  $\pi^+\pi^-\pi^+\pi^-\pi^0\pi^0$ ,  $\pi^+\pi^-\pi^+\pi^-\pi^+\pi^-$  production cross-sections in  $e^+e^-$  annihilation at  $(1.45 \div 1.80)$  GeV c.m. Energyproduction cross-sections in  $e^+e^-$  annihilation at  $(1.45 \div 1.80)$  GeV c.m. Energy», *Lett. Nuovo Cim.* **31**, 445 (1981).
- [55] C. Bacci *et al.*, «Measurement of hadronic exclusive cross sections in  $e^+e^-$  annihilation from 1.42 to 2.20 GeV», *Nucl. Phys. B* **184**, 31 (1981).
- [56] L.M. Kurdadze *et al.*, «Study of the reaction  $e^+e^- \rightarrow \pi^+\pi^-\pi^0\pi^0$  at  $(2 e)$  up to 1.4 GeV», *JETP Lett.* **43**, 643 (1986).
- [57] S.I. Dolinsky *et al.*, «Summary of experiments with the neutral detector at the  $e^+e^-$  storage ring VEPP-2M», *Phys. Rep.* **202**, 99 (1991).
- [58] M.N. Achasov *et al.*, « $e^+e^- \rightarrow 4\pi$  processes investigation in the energy range 0.98 GeV to 1.38 GeV with SND detector», 2001.
- [59] M. Ablikim *et al.*, «Measurement of the cross section for  $e^+e^- \rightarrow$  hadrons at energies from 2.2324 to 3.6710 GeV», arXiv:2112.11728 [hep-ex].
- [60] J.Z. Bai *et al.*, «Measurements of the Cross Section for  $e^+e^- \rightarrow$  Hadrons at Center-of-Mass Energies from 2 GeV to 5 GeV», *Phys. Rev. Lett.* **88**, 101802 (2002).
- [61] H.J. Behrend *et al.*, «A measurement of the  $\pi^0$ ,  $\eta$  and  $\eta'$  electromagnetic form-factors», *Z. Phys. C* **49**, 401 (1991).
- [62] J. Gronberg *et al.*, «Measurements of the meson-photon transition form-factors of light pseudoscalar mesons at large momentum transfer», *Phys. Rev. D* **57**, 33 (1998).
- [63] B. Aubert *et al.*, «Measurement of the  $\gamma\gamma^* \rightarrow \pi^0$  transition form factor», *Phys. Rev. D* **80**, 052002 (2009).
- [64] S. Uehara *et al.*, «Measurement of  $\gamma\gamma^* \rightarrow \pi^0$  transition form factor at Belle», *Phys. Rev. D* **86**, 092007 (2012).
- [65] C.F. Redmer, «Measurement of Meson Transition Form Factors at BESIII», *EPJ Web Conf.* **212**, 04004 (2019).
- [66] M. Hoferichter *et al.*, «Pion-Pole Contribution to Hadronic Light-by-Light Scattering in the Anomalous Magnetic Moment of the Muon», *Phys. Rev. Lett.* **121**, 112002 (2018).
- [67] Y. Guo, «Two photon physics at BESIII», *J. Phys.: Conf. Ser.* **1137**, 012008 (2019).
- [68] H. Czyż, P. Kisza, «EKHARA 3.0: An update of the EKHARA Monte Carlo event generator», *Comput. Phys. Commun.* **234**, 245 (2019).
- [69] M. Masuda *et al.*, «Study of  $\pi^0$  pair production in single-tag two-photon collisions», *Phys. Rev. D* **93**, 032003 (2016).